

## SUPPLEMENTAL INFORMATION

### Using Mitochondrial Activity to Select for Potent Human

### Hematopoietic Stem Cells

**Authors:** Jiajing Qiu <sup>1</sup>, Jana Gjini <sup>1,2</sup>, Tasleem Arif <sup>1</sup>, Kateri Moore <sup>1,2,3,4</sup>, Miao Lin <sup>1</sup>, and Saghi Ghaffari <sup>1,2,3,4,5,#</sup>

**Affiliations:** <sup>1</sup> Departments of Cell, Developmental & Regenerative Biology, <sup>2</sup> Graduate School of Biomedical Sciences, <sup>3</sup> Black Family Stem Cell Institute, <sup>4</sup> Tisch Cancer Institute, <sup>5</sup> Oncological Sciences, Icahn School of Medicine at Mount Sinai, New York, New York 10029

**# Correspondence:** Saghi Ghaffari, M.D.-Ph.D., Department of Cell, Developmental & Regenerative Biology, Icahn School of Medicine at Mount Sinai, New York, NY 10029, Tel: 212-659-8271, Fax: 212-803-6740; e-mail: [Saghi.Ghaffari@mssm.edu](mailto:Saghi.Ghaffari@mssm.edu)

## **SUPPLEMENTAL METHOD**

### **Image analysis**

2D confocal images were processed using ImageJ. 3D images were processed using Imaris 9.5.1 software.

### **Fluorescence intensity and nuclear size**

To determine the abundance of total cellular CDK6, TOM20 and DRP1 based on immunofluorescence, the integrated density in the channel displaying indicated fluorescence was measured on a per cell basis. Outline of nucleus was created by generating a binary image of DAPI. To measure the size of nuclear area, total number of pixels within nuclear outline was counted using analyze particles function. To measure the fluorescent intensity of CDK6 within the nucleus, the outline of nucleus was overlaid to the channel displaying CDK6 and the mean intensity within the overlay was measured. To determine the amount of localized DRP1 foci, a threshold was first applied and total fluorescent intensity of all areas of DRP1 above threshold were measured.

### **Colocalization**

Colocalization between TOM20 and DRP1 was analyzed using JACoP plug-in written for ImageJ. Auto threshold was applied and kept through all analyses unless otherwise specified. Mander's overlap coefficient was calculated to evaluate colocalization, measuring the fraction of fluorescent intensity of TOM20 in areas where the fluorescent intensity of DRP1 are above threshold.

### **Mitochondrial morphology**

Mitochondrial morphology of MMP-low or -high CD34<sup>+</sup>CD38<sup>-</sup> HSPCs was analyzed using the plug-in macro function MiNA (Mitochondrial Network Analysis) written for ImageJ 2D images. Auto threshold was applied to TOM20 or VDAC fluorescence intensity to generate the outline of mitochondria. Analyzing particle function was next applied to measure the size of individual mitochondrial fragment area. The average area size of all mitochondria fragments and content in each cell was calculated and compared between MMP- low and -high groups.

3D mitochondrial morphology of MMP-low or -high CD90<sup>+</sup> HSCs was analyzed using Imaris software. Surfaces of mitochondria were created based on the optimal signal to noise ratio and were applied to all acquired images. The total number of surfaces, the average volume and size of areas in each cell were compared between MMP-low and -high HSCs/HSPCs subpopulations.

### **Cell cycle analysis by Pyronin Y/Hoechst staining**

Sorted MMP-low or -high CD34<sup>+</sup>CD38<sup>-</sup> HSPCs or CD90<sup>+</sup> HSCs were first stained with Hoechst 33342 (20ug/ml, Invitrogen) at 37°C for 45 minutes in freshly prepared Hoechst Staining Medium (HSM; Hanks' buffered salt solution/10% FBS/20mM HEPES/1mg/ml Glucose/50ug/ml Verapamil) before Pyronin Y (1ug/ml, Sigma) was added and cells were stained for another 15 minutes. Cells were then washed, re-suspended in HSM containing 1ug/ml propidium iodide in HSM and analyzed by flow cytometry (BD Biosciences LSRII). Hoechst and Pyronin Y fluorescence were excited using UV laser and 488 laser respectively, and emission was collected with 480nm and 570nm filter respectively. The PY/HO profile of proliferating Jurkat T cells stained in parallel, which displayed a clear distribution of cell phases, was used as a reference for gate setting.

### **Human HSC transplantation into NSG mice**

Freshly sorted MMP-low or MMP-high CD90<sup>+</sup> HSCs from CB (800 cells per recipient mice) were transplanted via intravenous injection into NSG mice 8-9 weeks of age sub-lethally irradiated at 220 cGy (X-Ray source). Mice were given neomycin (Life Technology #21810031)/Polymycin B Sulfate (Sigma P1004) containing drinking water for totally 3 weeks starting 3 days prior to irradiation. PB was analyzed 3, 5, 7 months after transplantation. BM and spleen were harvested at the end of 7 months. To determine the chimerism (% human CD45 of total human and mouse CD45), MNCs of recipient PB, BM and spleen were stained with both human specific and murine specific anti-CD45 monoclonal antibodies and analyzed by flow cytometry. Lineage distribution was determined by staining with hCD33, hCD3, hCD19, and hCD235A (GlyA, Glycophorin A). Each analysis was paired with a corresponding matched unstained control.

### **Single cell kinetic analysis**

Single MMP-low or -high CD90<sup>+</sup> HSCs were sorted directly into 100ul serum free medium STEM SPAN (StemCell Technologies #09650) supplemented with 100ng/ml SCF (R&D Systems, 255-SC), 50nM/ml TPO (R&D Systems, 288-TP), 50ng/ml Flt3 ligand (R&D Systems, 308-FKN) in individual U-bottom wells of 96 well plates. Single cells were incubated at 37°C for 6 days. The occurrence of cell division in each well were scored under bright field microscopy every 12 hours. Cells were stained with DAPI at the end of culture to indicate viability. The wells containing undivided dead cells were excluded. To determine the kinetic of the first division, the cumulative percentage of all wells containing divided HSCs among total wells counted at each time point were plotted and fitted to sigmoidal curve by least squares fit. Time taken for cumulative 50% of cells to finish first division were determined as  $K_{half}$  of the curve. The percentage of de novo first division at each time point was fitted to a Spline curve. Time to the first and second division of each

cell were recorded to calculate the mean time of first division and mean interval time (the interval between the first and second division).

### **Bulk *ex vivo* culture for CDK6 expression or proliferation analysis**

MMP-low or -high CD90<sup>+</sup> HSCs [500 (for CDK6 immunostaining) or 150 (for proliferation analysis)] were cultured in U-bottom wells of 96-well plates in 200ul STEM SPAN supplemented with cytokines as above. The 500 cells bulk culture were harvested after 34 hrs and fixed for CDK6 immunostaining and confocal microscope study. The number of total live cells expanded from 150 seeded HSCs were counted after a 9-day incubation.

## **SUPPLEMENTAL FIGURES AND LEGENDS**

**Figure S1**

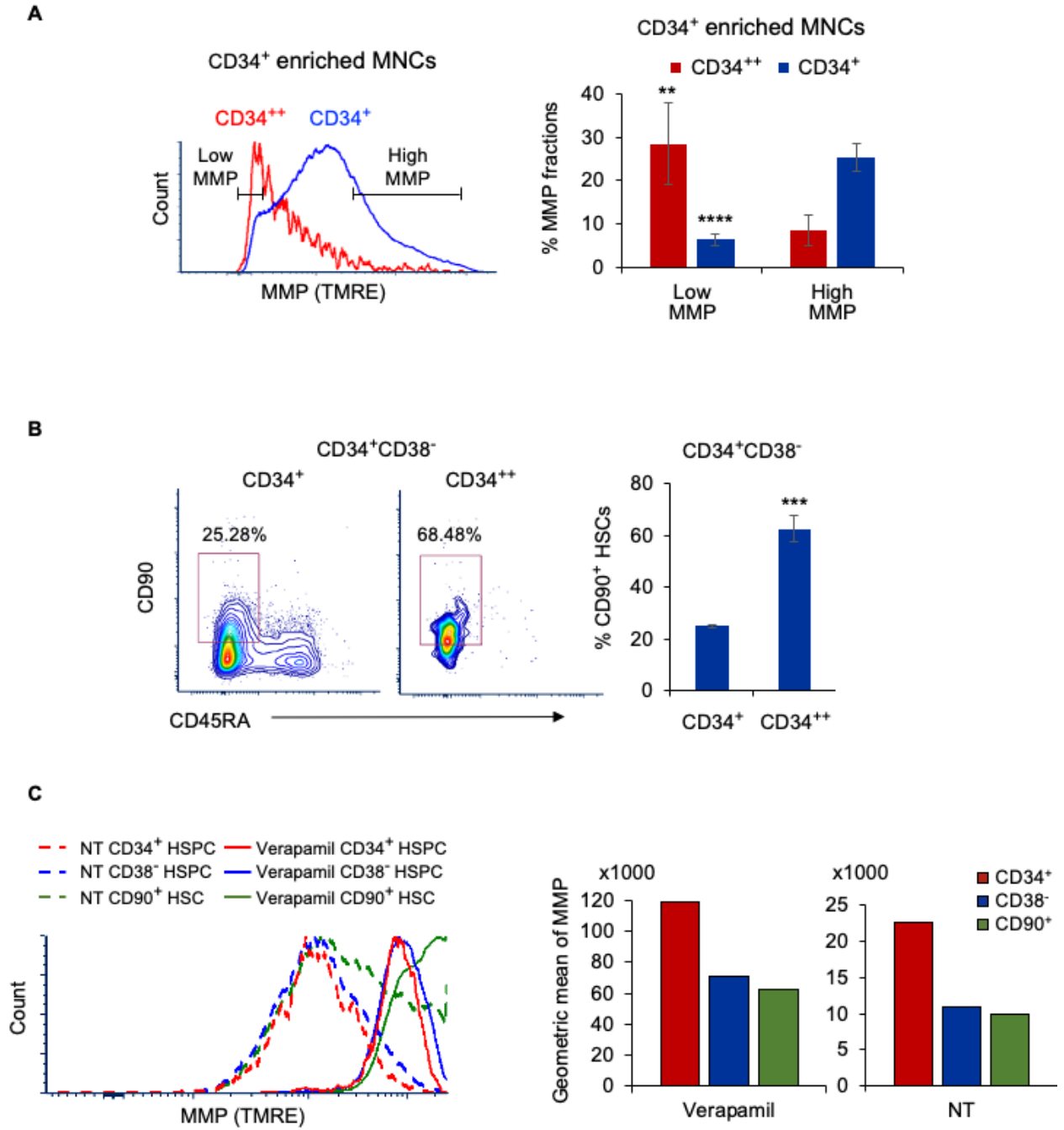


**Figure S1 A.** FACS histogram of MMP (left) and the percentage of low or high MMP (gated as in Figure 1) subset of total CD34<sup>+</sup> or CD34<sup>++</sup> fraction of CB MNCs (right; n=5). **B.** CD90/CD45RA FACS profiles (left) of total CD34<sup>+</sup> or CD34<sup>++</sup> fraction of CD38<sup>-</sup> CB HSPCs; The percentage of CD90<sup>+</sup> HSCs in parental populations (right; n=3). **C.** FACS histogram (left) of MMP of CD34<sup>+</sup> HSPCs, CD38<sup>-</sup> HSPCs, and CD90<sup>+</sup> HSCs of CB treated or non-treated (NT) with 50  $\mu$ M verapamil; Geometric means of fluorescence intensity of MMP (right). Data are presented as mean  $\pm$  SD; student's t-test: \*\*p < 0.01, \*\*\* p < 0.001, \*\*\*\*p < 0.0001.

**Figure S2**

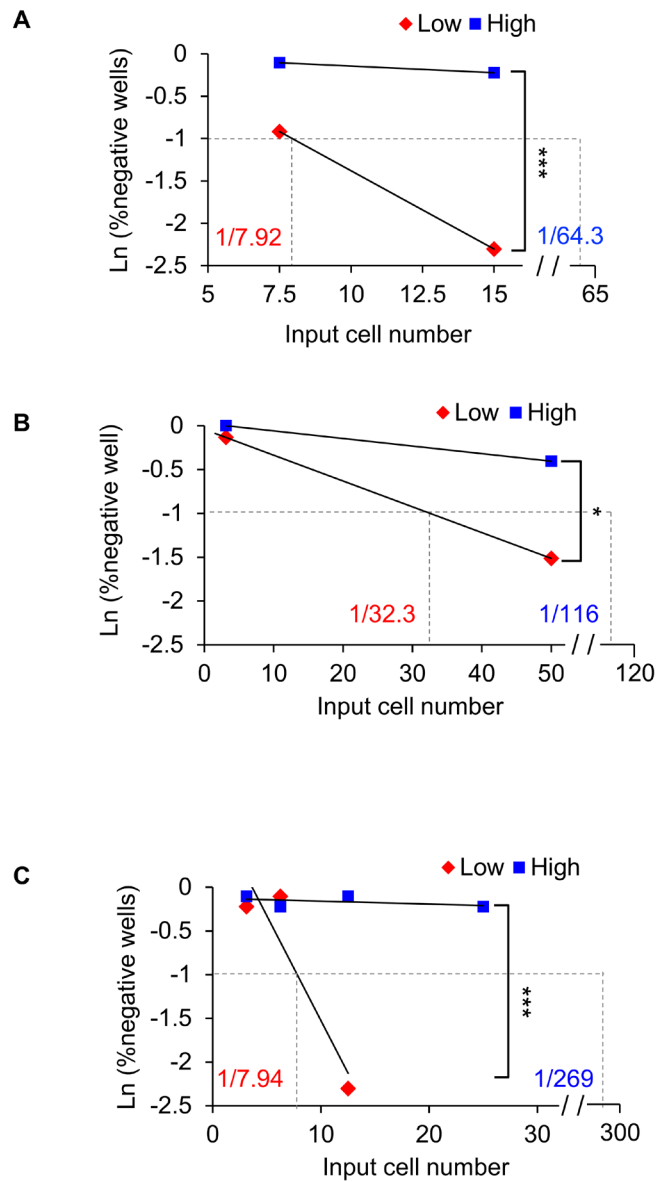


**Figure S2 A-C** Limiting dilution analysis of LTC-IC frequency in MMP-low and -high CD90<sup>+</sup> (A, C) and CD38<sup>-</sup> (B) PB HSCs in a 5 week (A, B) or 6.5-week (C) LTC. Dotted lines indicate LTC-IC frequency determined by - Ln 37% non-responder. p values calculated using L-Calc™ software. \*p < 0.05, \*\*\*p < 0.001.

**Figure S3 A**

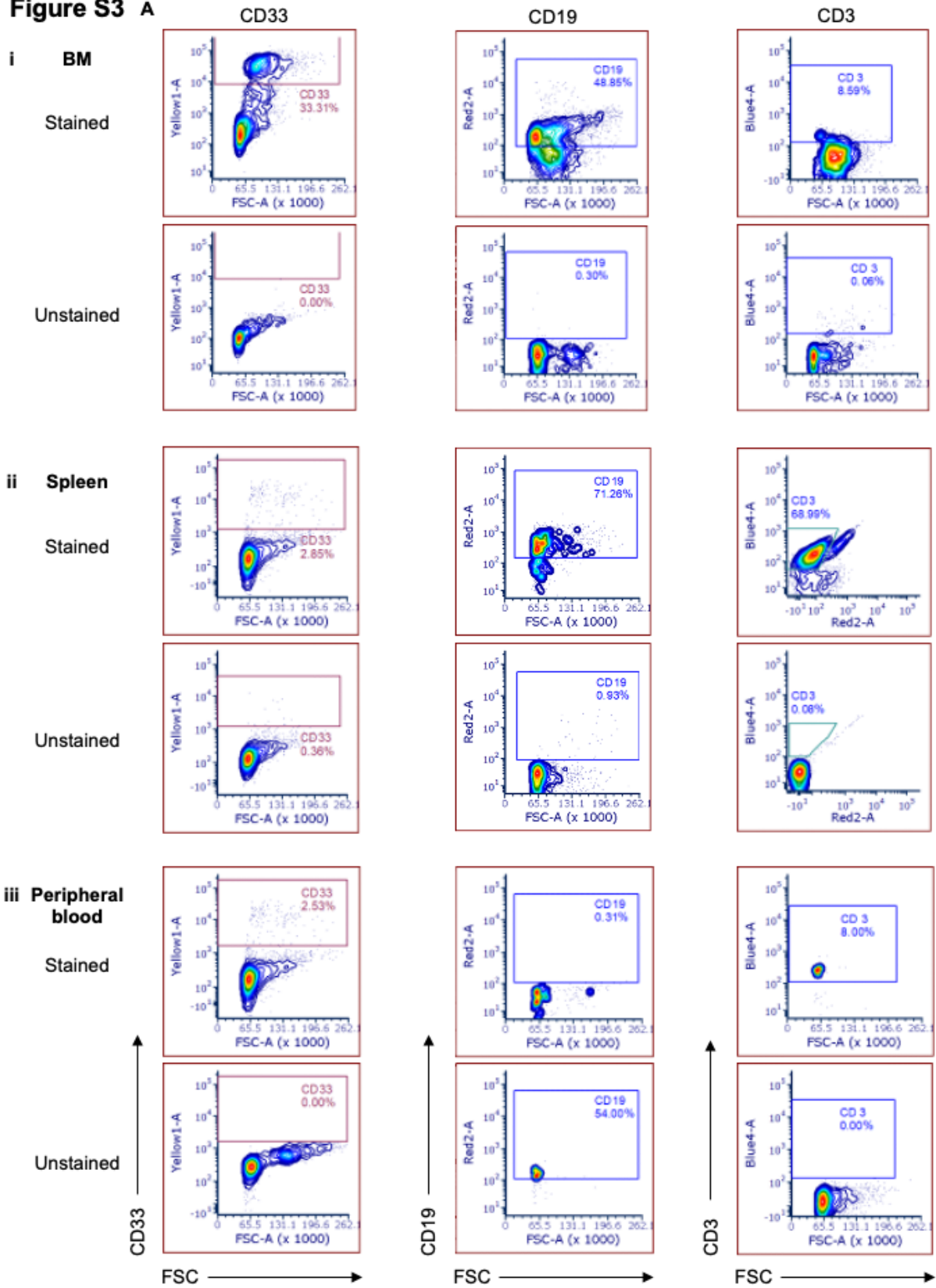




**Figure S3**

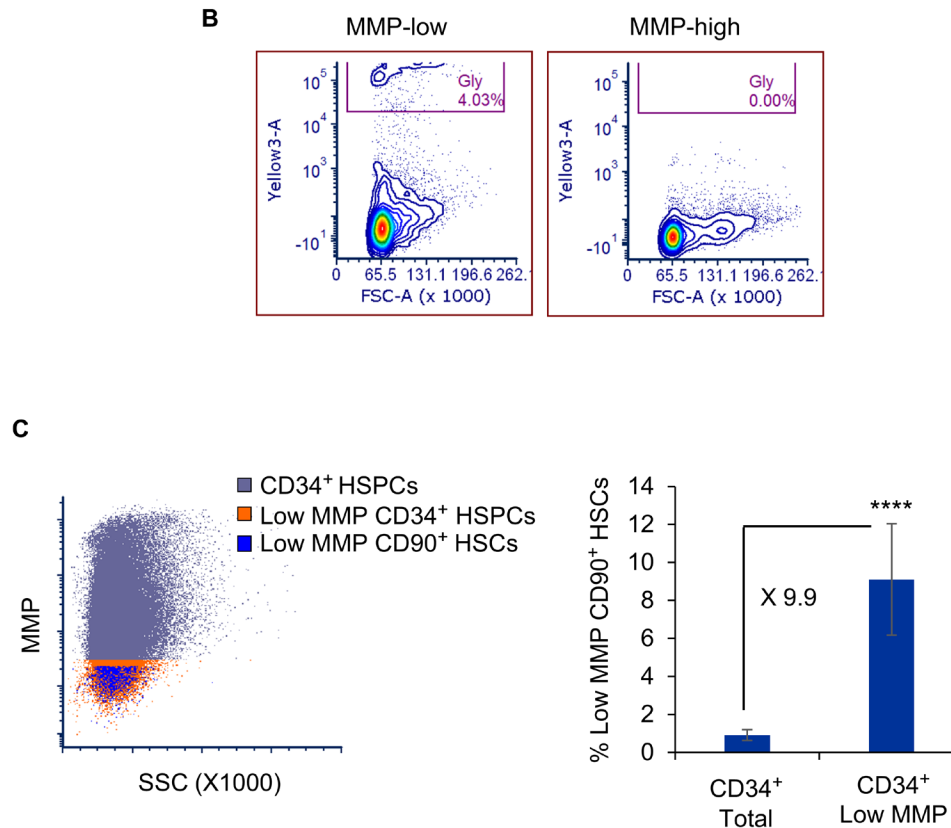


**Figure S3 A.** Representative FACS profiles of myeloid (CD33) and lymphoid (CD19, CD3) lineage markers (upper panels) and the corresponding unstained controls (lower panels) in BM (i), spleen (ii) and peripheral blood (iii) of NSG mouse recipients 7 months post-transplantation. **B.** Representative FACS profiles of human Glycophorin A (Gly) in hu-CD45<sup>-</sup> BM of NSG mouse transplanted with MMP-low or -high CD90<sup>+</sup> CB HSCs. **C.** FACS profile (left) of total CD34<sup>+</sup> cells, low MMP CD34<sup>+</sup> HSPCs, and low MMP CD90<sup>+</sup> HSCs of PB; Percentage of low MMP CD90<sup>+</sup> HSCs in total and in low MMP CD34<sup>+</sup> cells (right; n=5). Low MMP is gated according to 10% lowest MMP of CD90<sup>+</sup> HSCs as in Figure 1.

**Figure S4**

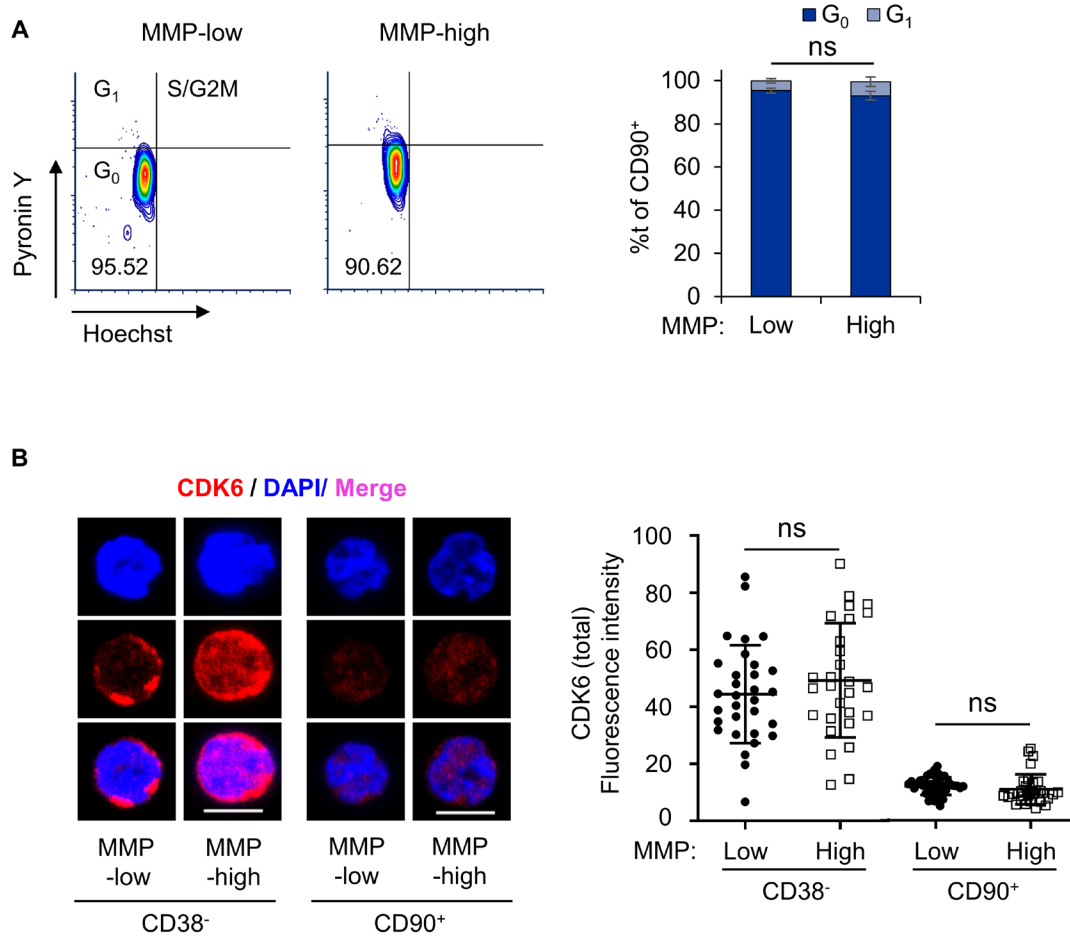


**Figure S4 A.** FACS profiles (left) of cell cycle analysis of sorted CD90<sup>+</sup> PB HSCs by Pyronin Y / Hoechst staining; Percentage of G<sub>0</sub> and G<sub>1</sub> in MMP-low or -high subsets (right; n=3). **B.** Representative immunofluorescent confocal image (left; scale bar: 5μm) and quantification (right) of total cellular immunofluorescence intensity of CDK6 in MMP -low and -high CD38<sup>-</sup> HSPCs and CD90<sup>+</sup> HSCs of PB. Data are represented as mean ± SD; student's t-test, ns. Not significant.

**Figure S5**

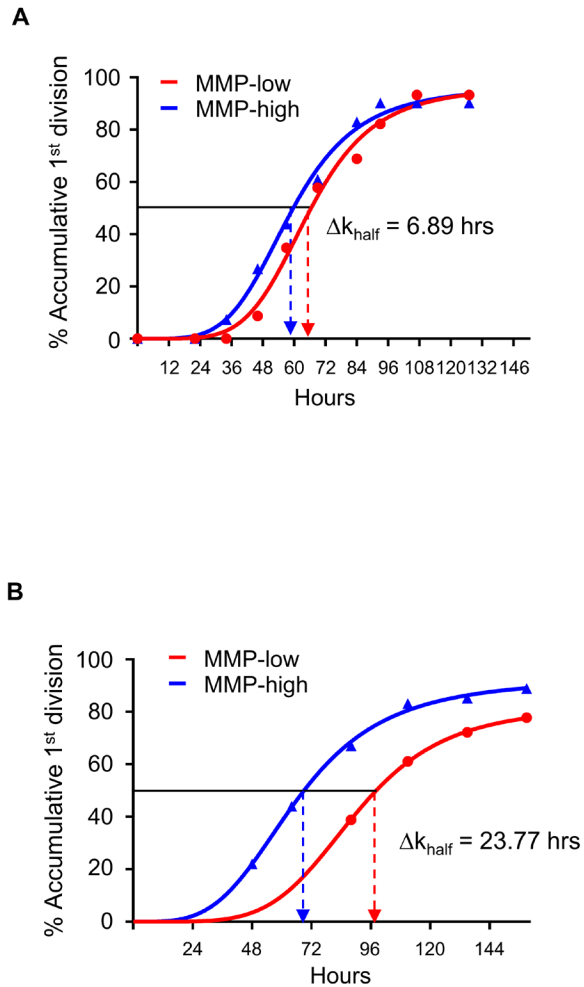


**Figure S5 A-B.** The percentage of cumulative first cell division (fitted into Sigmoidal curve) of MMP-low and -high CD38<sup>-</sup> PB HSC (**A**) or CD90<sup>+</sup> CB HSC (**B**) in single cell culture.  $R^2 > 0.99$ .  $K_{\text{half}}$ : hours for cumulative 50% of the cells to finish first division.  $\Delta K_{\text{half}}$ : Difference between  $K_{\text{half}}$  of MMP-low and -high cells.

**Figure S6**

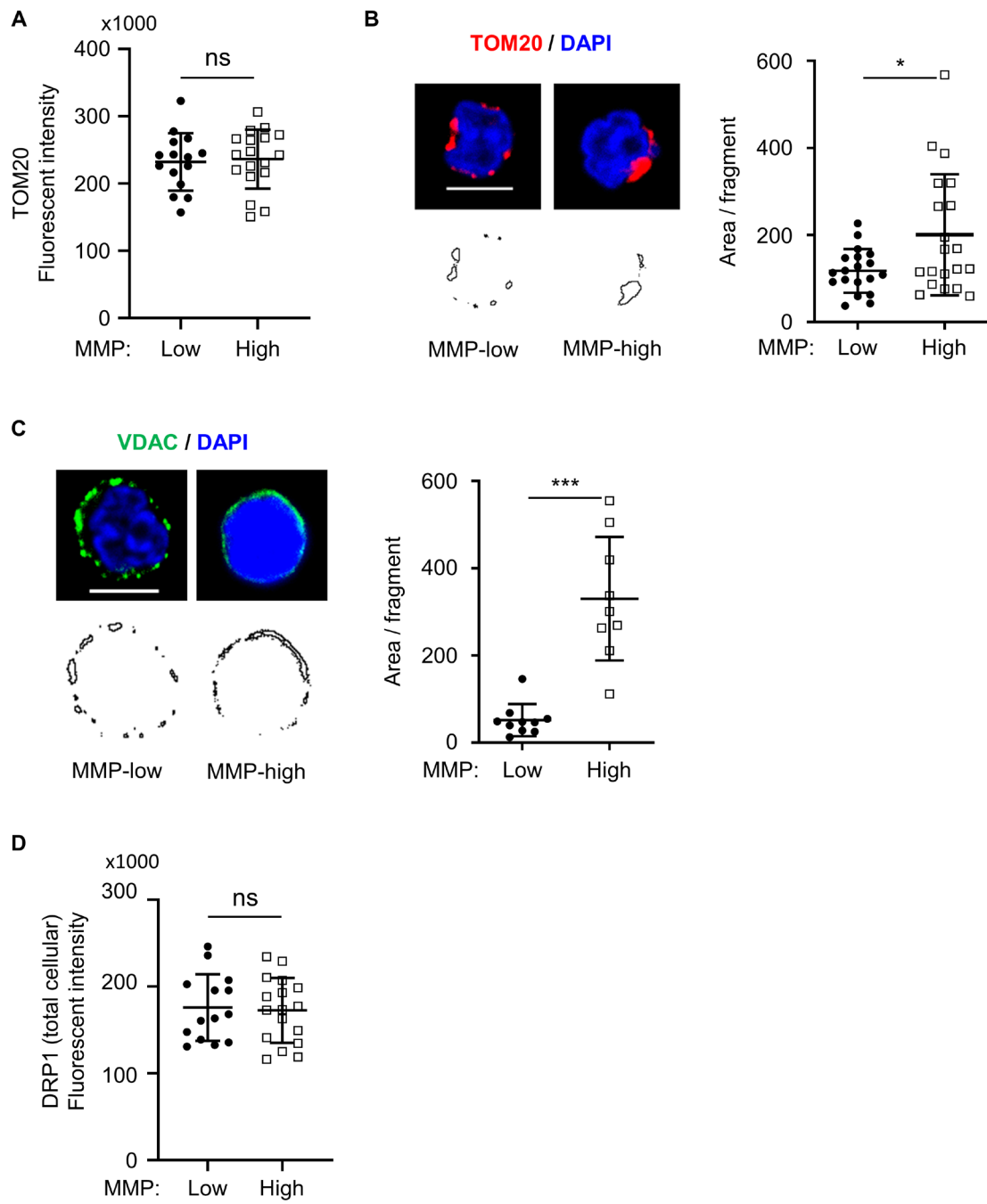


**Figure S6 A.** Total cellular fluorescence intensity of TOM20 in MMP-low or -high CD90<sup>+</sup> PB HSCs from combined z-stacks of 3D images. **B-C.** 2D immunofluorescent confocal images (left) of TOM20 (**B**) and VDAC (**C**) in MMP-low or -high CD38<sup>-</sup> PB HSPCs. Mitochondrial areas are outlined at bottom. Quantification of average area per mitochondrial fragment (right) labeled by TOM20 (**B**) or VDAC (**C**). **D.** Total cellular fluorescent intensity of DRP1 from combined z-stacks of 3D images. \*p < 0.05, \*\*\*p < 0.001.

## SUPPLEMENTAL TABLES

**TABLE S1: LTC-IC frequencies from limiting dilution analyses of 5-week human long-term cultures**

Experiment #	CD34 <sup>+</sup> CD38 <sup>-</sup> CD45RA <sup>-</sup> CD90 <sup>+</sup>			CD34 <sup>+</sup> CD38 <sup>-</sup>		
	MMP-Low	MMP-High	Fold change	MMP-Low	MMP-High	Fold change
1	7.75	54.22	7	17.72	64.35	3.6
2	7.92	64.30	8.12	32.33	116.71	3.6

**TABLE S2: ANTIBODIES**

<b>Flow cytometry</b>					
<b>Antibody</b>	<b>Source</b>	<b>Target</b>	<b>Host</b>	<b>Clone</b>	<b>Catalog #</b>
CD34 (APC)	BD Biosciences	Human	Mouse	581	555824
CD38 (PerCPCy5.5)	BD Biosciences	Human	Mouse	HIT2	561106
CD45RA (APCCy7)	Biologend	Human	Mouse	H100	304127
CD45RA-PECy7)	Biologend	Human	Mouse	H100	304125
CD90 (FITC)	BD Biosciences	Human	Mouse	5E10	555595
CD49f (PECy7)	eBiosciences	Human	Rat	eBR2a	25-0495-80
CD45 (APC)	BD Biosciences	Human	Mouse	HI30	560973
CD45 (FITC)	BD Biosciences	Human	Mouse	HI30	555482
CD45 (APC)	BD Biosciences	Mouse	Rat	30-F11	559864
CD3 (PerCPCy5.5)	BD Biosciences	Human	Mouse	UCHT1	560835
CD19 (Alexa Fluor 700)	BD Biosciences	Human	Mouse	HIB19	561031
CD33 (PE)	BD Biosciences	Human	Mouse	WM53	561816
<b>Immunofluorescence microscopy</b>					
<b>Antibody</b>	<b>Source</b>	<b>Host</b>	<b>Dilution</b>	<b>Catalog #</b>	
TOM20	Santa Cruz	Rabbit	1:100	sc-11415	
DLP1 (DRP1)	BD Trans. lab	Mouse	1:100	611112	
VDAC1/Porin	Abcam	Mouse	1:100	ab14734	
CDK6	Novus Biological	Rabbit	1:100	NBP1-87262	
Anti-Rabbit (Alexa Fluor 594)	Invitrogen	Goat	1:1000	A11012	
Anti-Mouse (Alexa Fluor 488)	Invitrogen	Goat	1:1000	A28175	